Published in final edited form as:

J Immunol. 2023 October 15; 211(8): 1240–1248. doi:10.4049/jimmunol.2200292.

Female But Not Male Mice Deficient in Soluble IgM are Susceptible to Chemically-Induced Glomerular Injury

Russell Whelan[*], **Andrew Feemster**[†], **Jennifer Laskowski**[†], **Brandon Renner**[†], **Liudmila Kulik**[†], **Felix Poppelaars**[†], **Cameron Lee**[†], **V. Michael Holers**[†], **Joshua M. Thurman**[†]

[*]Department of Pediatrics, University of Colorado School of Medicine, Anschutz Medical Campus, Aurora, CO, USA

[†]Department of Medicine, University of Colorado School of Medicine, Anschutz Medical Campus, Aurora, CO, USA

Abstract

B cell targeted therapies are effective for treating multiple different kidney diseases in humans and also protect mice from Adriamycin nephropathy. As glomerular IgM is frequently seen in both humans and mice with “non-immune” forms of glomerular disease, we hypothesized that natural IgM binds to epitopes displayed in the injured glomerulus, exacerbating injury. To test this hypothesis, we induced Adriamycin nephropathy in Balb/C mice that cannot secrete soluble IgM (*sIgM*$^{-/-}$ mice) and compared them to Balb/C controls. Contrary to our prediction, we found that female *sIgM*$^{-/-}$ mice developed higher mortality and more severe kidney injury after injection of Adriamycin. The absence of soluble IgM did not reduce glomerular complement activation, and IgG was seen deposited within the injured glomeruli. Furthermore, we discovered that female *sIgM*$^{-/-}$ mice have higher levels of anti-cardiolipin IgG, and that IgG from these mice binds to epitopes in the injured kidney. These findings indicate that natural IgM may prevent generation of auto-reactive IgG. Circulating levels of anti-cardiolipin IgG decreased after induction of kidney injury in female mice, consistent with deposition of the antibodies in injured tissues. Better understanding of the mechanisms by which the immune system modulates and amplifies kidney injury may enable the development of targeted therapies to slow kidney disease progression.

Introduction

Chronic kidney disease (CKD) is a major health problem that affects greater than 10% of the US population (1, 2). Unfortunately, once there is sufficient damage to the kidney ("the point of no return"), the glomerular filtration rate continues to decline even if the primary disease becomes quiescent (3-5). This suggests that kidney damage can trigger secondary pathologic processes, which then drive ongoing injury. Progressive deterioration in the function of diseased kidneys may be the result of hemodynamic factors and maladaptive functional

Corresponding author: Joshua M. Thurman, M.D., Division of Nephrology and Hypertension, C-281, 12700 E 19th Ave, Aurora, CO 80045, Phone: 303-724-7584, Fax: 303-724-7581, Joshua.Thurman@cuanschutz.edu.

Disclosure Statement

JMT and VMH are consultants for Q32 Bio, Inc., a company developing complement inhibitors. Both also hold stock and will receive royalty income from Q32 Bio, Inc.

changes in the remnant nephrons (6). The immune system may also play a role in disease progression, however, and tissue inflammation can amplify or prolong kidney injury after a self-limited insult.

We previously reported that natural antibodies bind to injured murine and human glomerular endothelial cells (GEnCs) (7). Natural antibody is immunoglobulin that is germline encoded and is produced even in the absence of specific antigen exposure (8). Natural antibodies are often self-reactive and can bind to epitopes displayed on the outer membrane of injured cells (9, 10). IgM and C3 deposits are frequently detected in kidney biopsies from patients with a diverse range of diseases, many of which are not thought of as immune-mediated (11-13). This suggests that natural IgM may bind to epitopes expressed or displayed within the glomerulus after non-immune injury. Although the IgM deposits are often attributed to “passive trapping” of the protein within the glomerulus, we have found that the associated complement deposits contain enzymatically activated complement fragments (7, 14). Immunoglobulin only activates complement when it is bound to cognate antigen, so this observation suggests that the glomerular immunoglobulin is bound to specific targets and is not merely trapped in the lesion.

B cell targeted drugs have emerged as effective therapies for a wide range of glomerular diseases. Interestingly, not all of these diseases are clearly antibody-mediated. Rituximab, for example, is effective for treatment of idiopathic nephrotic syndrome (15-17), a disease in which glomerular immune complexes are typically not seen. We have found that depletion of B cells is protective in several murine models of glomerular injury, including chemically induced podocyte injury (14, 18). B cells have multiple immunologic functions beyond the production of immunoglobulin, including production of cytokines as well as antigen presentation (19). Thus, B cells could play a role in kidney disease pathogenesis independent of antibody production. Furthermore, natural IgM has both pro- and anti-inflammatory functions. It helps the body to eliminate pathogens and facilitates the clearance of apoptotic cells (20), but it can also suppress some T and B cell functions (21). IgM deposits, therefore, could mediate either pathologic or protective effects.

Given the spectrum of functions performed by B cells and immunoglobulin, it is important to distinguish the contributions of various B cell subsets and IgM clones to disease pathogenesis. Greater understanding of the various roles that B cells and their products play in CKD progression will facilitate the development of therapies that effectively block the pathogenic processes. In the current study, we sought to specifically examine the role of IgM in a model of acquired glomerular injury. To selectively test whether glomerular IgM deposits are pathogenic in this model, we utilized mice with a targeted mutation in the μ_s exon (referred to as *sIgM*$^{-/-}$ mice) (22). These mice cannot secrete soluble IgM, although they can produce soluble forms of other immunoglobulin isotypes and other B cell functions are normal. We backcrossed the *sIgM*$^{-/-}$ mice onto a Balb/c background, as this strain is known to be susceptible to Adriamycin nephropathy (AN), a model of chemically induced podocyte injury that leads to progressive glomerular damage (23). We then tested whether the absence of soluble IgM affects the severity of kidney injury in this model.

Materials and Methods

Mice.

BALB/c were obtained from the Jackson Laboratory. *sIgM*$^{-/-}$ mice were generously provided by Kazue Takahashi (22), and were backcrossed for seven generations onto a Balb/c background. Western blot analysis confirmed that IgM was not detectable in the serum of these mice (Supplemental Figure 1). The following polymerase chain reaction (PCR) primers were used to screen the offspring. Wild-type allele: forward 5'- TGC ATC TGT CTT GCT TGC TC-3', reverse 5'- TCC TCC TCA GCA TTC ACC TC-3'. Knockout allele: forward 5'- CAA GAG AAG TAT GTG ACC AGT GC-3', reverse 5'- TCC TCC TCA GCA TTC ACC TC −3'. All mice were housed and maintained in the University of Colorado Center for Laboratory Animal Care in accordance with the *National Institutes of Health Guidelines for the Care and Use of Laboratory Animals*.

Adriamycin nephropathy.

The AN model was performed as previously described (6). Disease was induced in 9-12 week old mice with a single intravenous injection of 10 mg/kg of Adriamycin, (doxorubicin; Bedford Laboratories, Bedford, OH). Mice were followed for 1-4 weeks after injection with the Adriamycin. To examine binding of IgG within the injured kidney, wild-type BALB/c male mice were injected with either Adriamycin or vehicle as described above. On day 6, the mice were injected intravenously with equivalent amounts (600μg) of AlexaFluor-647-labeled IgG that had been purified from the serum of either male *sIgM*$^{-/-}$ (n=3) or female *sIgM*$^{-/-}$ (n=4) mice, with additional mice receiving PBS as a vehicle control (n=2). The mice were sacrificed 24 hours after injection of the labeled IgG, with serum and tissue collection at the time of sacrifice.

Kidney function measurements.

Glomerular filtration rate (GFR).—Mice were anesthetized with isofluorane and their backs were shaved. A MediBeacon GFR Monitor (St. Louis, MO) was secured on the shaved area. Mice were then retro-orbitally injected with FITC conjugated sinistrin (70 mg/kg) and housed singly for one hour. Data from monitors were collected, then analyzed using MediBeacon Software. Half-life of the FITC-sinistrin was measured between 15 minutes and 1-hour post-injection, and the half-life was then converted to μL/min.

Urine albumin measurement.—Urine albumin was measured by an enzyme linked immunosorbent assay (ELISA), according to the manufacturer's instructions (Bethyl Laboratories, Montgomery, TX). Urine creatinine was measured using a Creatinine Enzymatic Assay (Pointe Scientific Inc, Canton, MI). To normalize urine albumin excretion, the values are reported as micrograms albumin per milligram creatinine.

Histologic evaluation.

Kidneys were formalin fixed and paraffin embedded (FFPE). Three μm sections were cut and stained with periodic acid-Schiff (PAS). Slides were scanned using Aperio scanner. Using 20X magnification, borders were drawn manually around glomeruli by tracing

Bowman's capsule. The percentage of positive pixels and glomerular size were determined using ImageScope software (v.12.4.3.5008) with a 0.08 color threshold.

Fluorescence microscopy.—Kidneys were snap frozen in OCT compound (Sakura Finetek USA Inc., Torrance, CA) at the time of harvest and stored at −80°C until used. De-identified 5 μm tissue sections were warmed to room temperature, fixed in ice-cold absolute acetone for 5 minutes, washed twice in cold phosphate buffered saline (PBS). They were then blocked with 2% bovine serum albumin (BSA) and 5% heat-inactivated fetal bovine serum (HI FBS) in PBS for 2 hours at room temperature. Tissues were then stained with antibodies to C4, (0.5 μg/ml, clone 16D2, Hycult Biotech, Uden, The Netherlands), C3b (2 μg/ml; MP Biomedicals, Irvine, CA, USA), IgG Fcγ (5 μg/ml; Jackson Immuno, West Grove, PA, USA), MBL-C (2μg/mL, Hycult Biotech), or Type IV Collagen (25μg/mL rabbit polyclonal, EMD Biosciences, San Diego, CA, USA). Antibodies were diluted in PBS with 1% BSA and 2% HI-FBS and incubated on tissues overnight at 4°C or for 1 hour at room temperature. Slides were washed, mounted and sealed with ProLong Glass Mountant (Invitrogen) and imaged in a blinded fashion with an Olympus FV1000 FCS inverted confocal microscope (Olympus Life Science, Tokyo, Japan) at x100, x200, and x600 original magnification. Images were converted from binary data format and quantified with Olympus FV-10 ASW software (version 04.02.02.09). Quantification was performed on images collected at x100 magnification by region of interest (ROI) selection and measurement of area and fluor intensity in each specific channel. Quantified data are presented as pixel density per μm^2.

Terminal deoxynucleotidyl transferase dUTP nick end labeling (TUNEL) staining.—Kidney sections (12 μm) from female wild-type and *sIgM*$^{-/-}$ mice with Adriamycin nephropathy were stained using a TACS 2 TdT-Fluor *in situ* Apoptosis Detection Kit (Trevigen, Minneapolis, MN). The procedure was performed according to manufacturer's instructions. Four fields were captured at 20X magnification, and the number of glomeruli in each field were counted. Positively stained cells in the glomeruli and tubulointerstitium were counted in a blinded fashion. The average number of positive stained cells per glomerulus was then determined, and the total number of positive tubular cells per field was averaged for each sample.

Autoantibody measurements.

Anti-double stranded DNA (anti-dsDNA).—An Immunolon 2HB plate was coated with calf-thymus DNA (100 μg/mL, Sigma-Aldrich) in citrate buffer (0.15 M NaCl, 0.015 M sodium citrate, pH 8.0) and incubated overnight at room temperature. The plate was washed five times using PBS with 0.05% Tween 20 (PBST), and the plates were blocked with 1% BSA in PBST for one hour. Serum samples were serially diluted from 1:200 to 1:1600 in 1% BSA in PBST and then incubated on the plate overnight at 4°C. Anti-dsDNA antibodies were then detected with peroxidase conjugated goat anti-mouse IgG (H+L) (Jackson ImmunoResearch, West Grove, Pennsylvania) diluted 1:5000 in 1% BSA in PBST. Plates were then developed with 3,3',5,5'-tetramethylbenzidine (TMB) for 15 minutes, and the reaction was terminated with 0.2 M sulfuric acid. Absorbance was measured at 450 nm in triplicate.

Anti-cardiolipin ELISA.—IgG and IgM reactive with cardiolipin were detected using a mouse-specific protocol adapted from previously published methods (7, 24). Briefly, a nontreated polystyrene microtiter plate was coated with 50 μg/ml of cardiolipin from bovine heart (Sigma Aldrich, Darmstadt, Germany) diluted in absolute ethanol. The plate was incubated uncovered for 12-18 hours at 4°C with gentle rocking. It was then washed once with PBS, pH 7.4, gently blotted dry and then blocked with 10% active fetal bovine serum (FBS; Thermo-Fisher, Grand Island, New York) in PBS for at least one hour at RT. Serum samples were diluted in cold blocking buffer (1:10 for IgG and 1:50 for IgM), added to the ELISA plate, and incubated for one hour at 4°C. Plates were then washed three times. HRP-conjugated goat anti-mouse antibodies were then used to detect IgM (Southern Biotech, Birmingham, Alabama; 1:3000 dilution) and IgG (Jackson ImmunoResearch, West Grove Pennsylvania; 1:2500 dilution). The plates were then developed with 3,3',5,5'-tetramethylbenzidine (TMB) and the reaction was terminated with 0.2M sulfuric acid. The color change was measured at 450 nm.

Fluorescence measurements.—Sera from mice injected with fluorescently labeled IgG or PBS was diluted 2μL into 150μL of PBS, fluorescence in the sample was measured on a BioTek Synergy 2 (excitation-620/40nm; emission-680/30nm). Each sample was run in triplicate, with results were normalized to highest fluorescence readings.

Immunoglobulin purification.

For IgM purification, Balb/c mouse serum (Innovative Biological, Novi, MI) was diluted 1:10 in binding buffer (0.1M phosphate, 0.15M NaCl, pH 7.4) and passed over an anti-mouse IgM (μ chain) agarose column (Sigma, St. Louis, MO). The column was washed with 10 column volumes binding buffer, then the IgM was eluted with acidic buffer (0.1M glycine, sodium azide 0.02%, pH 2.3) and collected into neutralizing buffer (1M Tris-HCl, pH 9.0). The eluant was adjusted to a pH of 7 and buffer exchanged into PBS. To confirm the purity of the IgM, 1 μg of protein was resolved by electrophoresis on a 10% Tris-HCl gel (Bio-Rad, Hercules, CA). The gels were stained with Coomassie, or the proteins were transferred to a polyvinylidene fluoride membrane and probed with a goat anti-mouse IgM (μ-chain) antibody (Jackson ImmunoResearch).

For IgG purification, *sIgM*$^{-/-}$ mouse serum was collected and separately pooled from male and female mice, diluted 1:10 in binding buffer (0.1M phosphate, 0.15M NaCl, pH 7.4) and passed over anti-IgG (Protein G Sepharose 4) column (Sigma, St. Louis, MO). The column was washed with 10 column volumes binding buffer, then the IgG was eluted with acidic buffer (0.1M glycine, pH 2.) and collected into neutralizing buffer (1M Tris-HCl, pH 9.0). The eluant was adjusted to a pH of 7 and buffer exchanged into PBS. To confirm the purity of the IgG, 1 μg of protein was resolved by electrophoresis on a 10% Tris-HCl gel (Bio-Rad, Hercules, CA). and stained with Coomassie. Purified IgG was labeled with AlexaFluor-647 (Invitrogen) according to the manufacturer's instructions. The final concentration of IgG and the fluorophore labeling efficiency were determined by spectrophotometer (Nanodrop).

Flow Cytometry.

To examine binding of immunoglobulin to glomerular endothelial cells, immortalized murine cells were grown in tissue culture flasks to confluency (25). Cells were detached from the flasks with Accutase (Innovative Cell Technologies, San Diego, CA) and washed in PBS. Then, 0.5×10^6 cells were suspended in 50-μL PBS containing 10% mouse sera. The mixture was incubated on ice for 1 h and then gently vortexed every 20 min to keep the cells in suspension. Cells were then washed with PBS and incubated for 1 hour at 4°C in 50-μL DyLight 650 anti-mouse IgG, diluted 1:200. Cells were again washed, and fluorescence was then measured using a Cytek Aurora flow cytometer. Approximately 300,000 events were collected for each sample, and the results were analyzed using FlowJo software.

Electron microscopy.

Tissue samples were fixed overnight with 2.5% (v/v) glutaraldehyde in 0.1M sodium cacodylate buffer. After five rinses in 0.1M sodium cacodylate buffer, they were postfixed in 1% osmium tetroxide and 0.8% Potassium Ferrocyanide in 0.1M sodium cacodylate buffer for 1.5 hours. Tissue samples were then rinsed five times in water and en bloc stained with 2% uranyl acetate in 50% Ethanol for 2 hours. Then they were dehydrated with increasing concentrations of ethanol, transitioned into resin with propylene oxide, infiltrated with EMbed-812 resin and polymerized in a 60°C oven overnight. Blocks were sectioned with a diamond knife (Diatome) on a Reichert ultramicrotome and collected onto copper grids, post stained with 2% aqueous uranyl acetate and lead citrate. Images were acquired on a Tecnai T12 transmission electron microscope (Thermo Fisher) equipped with a LaB_6 source at 80kV using a XR80 (8Mpix) camera (AMT).

Statistical analysis.

Data were analyzed using GraphPad Prism software (GraphPad Prism, La Jolla, CA). Comparisons between two groups were performed using unpaired *t*-test. Multiple group comparisons were performed by analysis of variance (ANOVA) with post hoc Tukey's *t*-test. Log rank analyses were performed to compare survival. A P-value of less than 0.05 was considered statistically significant.

Results

Female *sIgM*$^{-/-}$ mice are more susceptible to Adriamycin nephropathy than wild-type controls.

AN was induced with a single intravenous injection of Adriamycin, and mice were initially followed for four weeks. Mortality over the follow-up period was greater in the *sIgM*$^{-/-}$ mice than in controls, and it was particularly high in the female *sIgM*$^{-/-}$ mice (Figure 1 A-B). The mortality increased during the second week post-Adriamycin. Therefore, kidney function and albuminuria were analyzed in samples collected one-week post-injection to avoid survival bias. The measured GFR at week 1 was already significantly lower in the *sIgM*$^{-/-}$ mice than in controls (Figure 1C), and this difference was primarily driven by a fall in the GFRs of female *sIgM*$^{-/-}$ mice (Figure 1D). Albuminuria in the male and female *sIgM*$^{-/-}$ mice was not significantly different than that in wild-type mice (Figure 1 E-F).

Female *sIgM*$^{-/-}$ mice develop more severe histologic injury than female wild-type mice.

AN causes injury to podocytes in Balb/c mice, leading to glomerulosclerosis and tubulointerstitial injury (26). We examined histologic injury in the kidneys of *sIgM*$^{-/-}$ and wild-type mice 1 week after injection with adriamcyin (Figure 2A). Images were scanned, and the percentage of each glomerulus that stained positively for PAS was analyzed as an indicator of extracellular matrix deposition. We also measured the average size of each glomerulus. Glomeruli in kidneys from the *sIgM*$^{-/-}$ mice had a greater percentage of PAS-positive material (Figure 2B), and the average glomerular size was also greater compared to wild-type control mice (Figure 2C).

IgG and complement proteins are deposited in the glomeruli of *sIgM*$^{-/-}$ mice with AN.

We previously found that B cell deficiency is associated with reduced glomerular immunoglobulin and complement deposits at four weeks post-Adriamycin (14). Those results, as well as analysis of human tissues (7), suggest that IgM can activate the classical pathway within damaged glomeruli. We analyzed glomerular IgG in the *sIgM*$^{-/-}$ and control mice one week after injection with Adriamycin, and found that the abundance of glomerular IgG was increased in both strains compared to vehicle injected control mice (Figure 3).

Our previous study showed that glomerular C4 was reduced in B cell deficient mice (14). In the current study, however, we found complement proteins C3b and C4 were deposited in the glomeruli of *sIgM*$^{-/-}$ and control mice with AN. The pattern of glomerular C4 was similar to that of glomerular IgG (Figure 3A). Thus, it is likely that IgG activates the classical pathway within the glomeruli after injury. MBL-C was deposited in glomeruli of both wild-type and *sIgM*$^{-/-}$ females treated with Adriamycin, indicating that the lectin pathway is also activated in this model (Supplemental Figure 2). We also previously found that tubulointerstitial complement activation is predominantly mediated by the alternative pathway in this model (27). Consistently, IgM deficiency did not have any impact on tubulointerstitial C3b deposition (Figure 3C). These results indicate that the classical pathway is engaged by IgG within injured glomeruli, whereas the alternative pathway is activated in the damaged tubulointerstitium. Furthermore, soluble IgM is not required for either of these processes.

We also examined the kidneys of wild-type and *sIgM*$^{-/-}$ mice by electron microscopy. Compared to vehicle-only treatment, podocytes of both strains of mice demonstrated significant injury after treatment with Adriamycin. There was foot process effacement and fewer open capillary loops (Figure 4). Podocytes also demonstrated classic hallmarks of cell death, including peripheral nuclear condenstion and swelling of electron-dense mitochondria (Supplemental Figure 3). Subepithelial electron-dense deposits were also seen in glomeruli of female *sIgM*$^{-/-}$ mice (Figure S2B). Of note, these humps were seen in female mice treated with either Adriamycin or vehicle, but were rarely observed in the glomeruli of wild-type mice micrographs.

IgM does not protect the kidneys from injury in AN.

The greater degree of mortality and kidney injury in the *sIgM*$^{-/-}$ mice with AN could be due to a protective function of IgM that is absent in these mice. It has been shown, for

example, that natural IgM helps the body to clear apoptotic cells in a non-inflammatory fashion (28). To examine whether clearance of apoptotic cells was impaired in *sIgM*$^{-/-}$ mice, we performed TUNEL staining on kidney sections from female mice with AN (Figure 5A). TUNEL-positive cells were seen in the glomeruli and tubulointerstitium of both wild-type and *sIgM*$^{-/-}$ mice with AN, and there was a trend towards fewer TUNEL-positive cells in the *sIgM*$^{-/-}$ mice (Figure 5A). Similarly, cleaved caspase-3 staining was not increased in the glomeruli of any of the treatment conditions (Supplemental Figure 4). Therefore, impaired clearance of apoptotic cells does not explain the greater degree of injury in these mice.

We also examined whether reconstitution of *sIgM*$^{-/-}$ mice with IgM would restore protection in this model. IgM was purified from wild-type Balb/c serum, and *sIgM*$^{-/-}$ mice were injected intraperitoneally with 1 mg of IgM one hour before induction of AN. There was a trend towards greater mortality in the mice injected with IgM compared to control mice during the first week after injection with Adriamycin (Figure 5C), and injection of the mice with IgM did not have a significant effect on GFR or albuminuria at this timepoint. These findings argue against a substantial protective role for natural IgM in this model.

Auto-reactive IgG antibody levels are higher in female *sIgM*$^{-/-}$ mice compared to male *sIgM*$^{-/-}$ mice and wild-type controls.

As we could not detect a protective role for IgM, we next considered whether the absence of soluble IgM in the *sIgM*$^{-/-}$ mice led to compensatory changes that might exacerbate injury. Production of soluble IgM has been reported to prevent the development of IgG anti-dsDNA antibodies (29, 30). To test the possibility that autoreactive IgG exacerbates injury in the *sIgM*$^{-/-}$ mice, we measured levels of anti-dsDNA antibodies in the serum of experimental mice. Baseline levels were similar in *sIgM*$^{-/-}$ and wild-type Balb/c mice. Interestingly, the level of anti-dsDNA antibody in the *sIgM*$^{-/-}$ mice consistently fell after induction of kidney injury (Figure 6A).

We previously found that a natural IgM clone that binds to cardiolipin also binds to injured glomerular endothelial cells (7, 18). Therefore, we examined levels of anti-cardiolipin IgM in wild-type and *sIgM*$^{-/-}$ mice using a cardiolipin ELISA. The levels of anti-cardiolipin IgM in wild-type mice increased after Adriamycin injection (Figure 5B), indicating that the mice produce more of the nephritogenic antibody in response to disease. Levels in male and female wild-type mice were not significantly different. As expected, the levels of anti-cardiolipin IgM in *sIgM*$^{-/-}$ mice were below the limit of detection. It has been reported that natural IgG anti-cardiolipin antibodies correlate with long-term allograft failure in kidney transplant recipients (31), suggesting that anti-cardiolipin IgG can also be an important mechanism of chronic kidney damage. We also measured IgG anticardiolipin antibodies and found that they were higher in vehicle-treated female *sIgM*$^{-/-}$ mice compared to male mice or wild-type controls (Figure 6D). As with the anti-dsDNA antibodies, levels of IgG anticardiolipin antibodies in female *sIgM*$^{-/-}$ mice fell after treatment with Adriamycin.

The fall in autoantibody levels in female *sIgM*$^{-/-}$ mice after injection with Adriamycin is more likely due to deposition of the antibodies in tissues than to a decrease in antibody production, given the timeframe in which it occurs. To test whether IgG autoantibodies bind to kidney cells, we performed an experiment in which murine glomerular endothelial cells

were detached and then exposed to serum. A greater amount of IgG bound to the cells after treatment with serum from control female *sIgM*$^{-/-}$ mice compared to serum collected from mice one week after injection with Adriamycin (Figure 6E). This finding strongly indicates there is reactivity of IgG present in the serum of female *sIgM*$^{-/-}$ mice towards epitopes on glomerular endothelial cells.

In another experiment, we purified IgG from the serum of male and female *sIgM*$^{-/-}$ mice and fluorescently labeled it with AlexaFluor 647. We then intravenously injected the labeled IgG into wild-type mice treated with Adriamycin. The mice were sacrificed 24 hours later, and we examined the kidneys by fluorescence microscopy. IgG purified from female *sIgM*$^{-/-}$ mice was deposited in the glomeruli and proximal tubules (Figure 6F). In contrast, only small amounts of IgG were seen in the tubules of mice with AN that had received IgG purified from the serum of male *sIgM*$^{-/-}$ mice. Circulating levels of the injected IgG were examined by measuring fluorescence of the serum. The levels of IgG that had been purified from female *sIgM*$^{-/-}$ mice were lower compared to the levels of IgG purified from male *sIgM*$^{-/-}$ mice (Figure 6G). This suggests greater target-mediated clearance, or deposition in tissues, of IgG from the female mice.

Discussion

In this study, we tested whether deficiency of soluble IgM protects mice from chemically induced glomerular injury. B cell depleting therapies are now used to treat many forms of glomerular disease, and our previous work showed that B cell deficiency is associated with milder glomerular disease in several models, including AN (14, 18). As IgM is frequently deposited in the kidneys of mice and humans with acquired kidney injury, we hypothesized that natural IgM reactive with glomerular injury epitopes is a mechanism of secondary injury in this model. *sIgM*$^{-/-}$ mice develop B cells and can produce immunoglobulin, including cell surface IgM, but they do not produce soluble IgM (22). Consequently, this strain of mice allowed us to specifically examine the role of glomerular IgM deposits in AN, independent of other B cell functions. Male *sIgM*$^{-/-}$ mice were not protected in this model. Surprisingly, we found that female *sIgM*$^{-/-}$ mice developed more severe disease compared to wild-type controls. They developed worse kidney injury within one week post injection with Adriamycin, and they displayed greater mortality over four weeks.

Previous studies have shown that *sIgM*$^{-/-}$ mice produce higher levels of anti-dsDNA antibodies than control mice (30), so we examined whether the congenital absence of IgM leads to autoantibodies, which might then amplify or sustain glomerular injury caused by Adriamycin. The level of anti-dsDNA antibodies was similar in *sIgM*$^{-/-}$ and control mice. We have previously found that natural IgM reactive with cardiolipin exacerbates glomerular injury (14, 18). In the current study, female mice deficient in soluble IgM had higher levels of anti-cardiolipin IgG than male *sIgM*$^{-/-}$ mice or wild-type controls. The level of anti-cardiolipin IgG in the serum of female *sIgM*$^{-/-}$ mice fell after treatment with Adriamycin, suggesting that AN creates an “antigen sink” for the antibodies. A greater amount of IgG in the serum of these mice bound to glomerular endothelial cells compared to male mice or wild-type controls. Furthermore, IgG purified from the serum of female *sIgM*$^{-/-}$ mice bound to kidney surfaces when injected into mice with AN. In addition, IgG derived from

female *sIgM*$^{-/-}$ mice demonstrated rapid clearance from the bloodstream, consistent with the increased IgG deposition in renal tissue. Conversely, IgG purified from male *sIgM*$^{-/-}$ mice was less evident within the kidneys and persisted longer in the circulation. Thus, production of auto-reactive IgM may prevent generation of pathogenic auto-reactive IgG, and these autoantibodies bind to neoepitopes expressed in the damaged kidney. Furthermore, high levels of self-reactive IgG may be even more deleterious than self-reactive IgM, given that female *sIgM*$^{-/-}$ mice developed more severe disease than wild-type control mice. The observation of enhanced antibody-mediated injury in females aligns with the well-established concept of sexual dimorphism in humoral immune responses.

It is possible that *sIgM*$^{-/-}$ mice develop more severe injury because natural IgM attenuates acquired injury. Studies have shown, for example, that natural IgM has some homeostatic and anti-inflammatory functions (20). We did not see evidence of protection when *sIgM*$^{-/-}$ mice were reconstituted with IgM purified from wild-type mice, and there was actually a trend towards greater mortality in these mice. Natural IgM also facilitates the clearance of apoptotic cells (20), but we did not see increased numbers of apoptotic cells in the kidneys of *sIgM*$^{-/-}$ mice with AN.

Our study has several limitations. First, it is possible that there are other IgG autoantibodies or natural antibodies, beyond anti-ds DNA and anti-cardiolipin, that are increased in the *sIgM*$^{-/-}$ mice. The current study also does not rule out the possibility that IgM is an important part of this process, but the results demonstrate that the absence of some B cell subsets or IgM species may induce compensatory changes that can exacerbate injury. It is interesting that the effect was primarily seen in female mice. There is experimental evidence showing that the natural antibody repertoire is different in females compared with males (32), and future experiments can examine the cellular and molecular differences in the immune system of these mice that make them more susceptible to injury. This, in turn, could lead to the discovery of new immune-mediated mechanisms of kidney injury.

In conclusion, we found that female *sIgM*$^{-/-}$ mice develop more severe mortality and kidney injury after injection with Adriamycin. The greater degree of kidney injury was associated with higher levels of pre-existing anti-cardiolipin IgG, with evidence of deposition of IgG on kidney tissue in both culture and animal studies. These findings indicate that auto-reactive IgG may bind to injury-epitopes within the damaged glomerulus and exacerbate injury. Our results also demonstrate that soluble IgM attenuates the production of this auto-reactive antibody. B cell targeted therapies are now used for a wide range of kidney diseases, including some that are thought to be antibody-mediated (33, 34) as well as diseases whose pathogenesis is incompletely understood (15). Our results demonstrate that different B cell subsets may play conflicting roles in the progression of kidney disease, highlighting the need for better understanding of these diseases and more targeted therapies.

Supplementary Material

Refer to Web version on PubMed Central for supplementary material.

Acknowledgments

This work was supported by National Institutes of Health Grants R01DK076690 and R01DK113586 (JMT), and R01DK125823 (JMT and VMH).

References.

1. Levey AS, Stevens LA, Schmid CH, Zhang YL, Castro AF 3rd, Feldman HI, Kusek JW, Eggers P, Van Lente F, Greene T, Coresh J, and E. P. I. Ckd. 2009. A new equation to estimate glomerular filtration rate. Annals of internal medicine 150: 604–612. [PubMed: 19414839]
2. Murphy D, McCulloch CE, Lin F, Banerjee T, Bragg-Gresham JL, Eberhardt MS, Morgenstern H, Pavkov ME, Saran R, Powe NR, Hsu CY, C. Centers for Disease, and T. Prevention Chronic Kidney Disease Surveillance. 2016. Trends in Prevalence of Chronic Kidney Disease in the United States. Ann Intern Med 165: 473–481. [PubMed: 27479614]
3. Remuzzi G, Benigni A, and Remuzzi A. 2006. Mechanisms of progression and regression of renal lesions of chronic nephropathies and diabetes. J Clin Invest 116: 288–296. [PubMed: 16453013]
4. Davidson A 2016. What is damaging the kidney in lupus nephritis? Nature reviews. Rheumatology 12: 143–153. [PubMed: 26581344]
5. Maschio G, Oldrizzi L, and Rugiu C. 1991. Is there a “point of no return” in progressive renal disease? J Am Soc Nephrol 2: 832–840. [PubMed: 1751786]
6. Ruiz-Ortega M, Rayego-Mateos S, Lamas S, Ortiz A, and Rodrigues-Diez RR. 2020. Targeting the progression of chronic kidney disease. Nature reviews. Nephrology 16: 269–288. [PubMed: 32060481]
7. Trachtman H, Laskowski J, Lee C, Renner B, Feemster A, Parikh S, Panzer SE, Zhong W, Cravedi P, Cantarelli C, Kulik L, You Z, Satchell SC, Rovin B, Liu F, Kalled SL, Holers VM, Jalal D, and Thurman JM. 2021. Natural Antibody and Complement Activation Characterize Patients with Idiopathic Nephrotic Syndrome. Am J Physiol Renal Physiol.
8. Ehrenstein MR, and Notley CA. 2010. The importance of natural IgM: scavenger, protector and regulator. Nat Rev Immunol 10: 778–786. [PubMed: 20948548]
9. Peng Y, Kowalewski R, Kim S, and Elkon KB. 2005. The role of IgM antibodies in the recognition and clearance of apoptotic cells. Mol Immunol 42: 781–787. [PubMed: 15829266]
10. Zwart B, Ciurana C, Rensink I, Manoe R, Hack CE, and Aarden LA. 2004. Complement activation by apoptotic cells occurs predominantly via IgM and is limited to late apoptotic (secondary necrotic) cells. Autoimmunity 37: 95–102. [PubMed: 15293879]
11. Ainsworth SK, Hirsch HZ, Brackett NC Jr., Brissie RM, Williams AV Jr., and Hennigar GR. 1982. Diabetic glomerulonephropathy: histopathologic, immunofluorescent, and ultrastructural studies of 16 cases. Hum Pathol 13: 470–478. [PubMed: 7042531]
12. Gamble CN 1986. The pathogenesis of hyaline arteriolosclerosis. Am J Pathol 122: 410–420. [PubMed: 2420184]
13. Mujais SK, Emmanouel DS, Kasinath BS, and Spargo BH. 1985. Marked proteinuria in hypertensive nephrosclerosis. American journal of nephrology 5: 190–195. [PubMed: 3160240]
14. Strassheim D, Renner B, Panzer S, Fuquay R, Kulik L, Ljubanovic D, Holers VM, and Thurman JM. 2013. IgM Contributes to Glomerular Injury in FSGS. J Am Soc Nephrol 24: 393–406. [PubMed: 23393315]
15. Ravani P, Lugani F, Drovandi S, Caridi G, Angeletti A, and Ghiggeri GM. 2021. Rituximab vs Low-Dose Mycophenolate Mofetil in Recurrence of Steroid-Dependent Nephrotic Syndrome in Children and Young Adults: A Randomized Clinical Trial. JAMA Pediatr 175: 631–632. [PubMed: 33616641]
16. Basu B, Sander A, Roy B, Preussler S, Barua S, Mahapatra TKS, and Schaefer F. 2018. Efficacy of Rituximab vs Tacrolimus in Pediatric Corticosteroid-Dependent Nephrotic Syndrome: A Randomized Clinical Trial. JAMA Pediatr 172: 757–764. [PubMed: 29913001]
17. Ravani P, Rossi R, Bonanni A, Quinn RR, Sica F, Bodria M, Pasini A, Montini G, Edefonti A, Belingheri M, De Giovanni D, Barbano G, Degl'Innocenti L, Scolari F, Murer L, Reiser J, Fornoni

A, and Ghiggeri GM. 2015. Rituximab in Children with Steroid-Dependent Nephrotic Syndrome: A Multicenter, Open-Label, Noninferiority, Randomized Controlled Trial. J Am Soc Nephrol.

18. Panzer SE, Laskowski J, Renner B, Kulik L, Ljubanovic D, Huber KM, Zhong W, Pickering MC, Holers VM, and Thurman JM. 2015. IgM exacerbates glomerular disease progression in complement-induced glomerulopathy. Kidney Int 88: 528–537. [PubMed: 25945405]
19. Lee DSW, Rojas OL, and Gommerman JL. 2021. B cell depletion therapies in autoimmune disease: advances and mechanistic insights. Nat Rev Drug Discov 20: 179–199. [PubMed: 33324003]
20. Chen Y, Park YB, Patel E, and Silverman GJ. 2009. IgM antibodies to apoptosis-associated determinants recruit C1q and enhance dendritic cell phagocytosis of apoptotic cells. J Immunol 182: 6031–6043. [PubMed: 19414754]
21. Lobo PI, Bajwa A, Schlegel KH, Vengal J, Lee SJ, Huang L, Ye H, Deshmukh U, Wang T, Pei H, and Okusa MD. 2012. Natural IgM anti-leukocyte autoantibodies attenuate excess inflammation mediated by innate and adaptive immune mechanisms involving Th-17. J Immunol 188: 1675–1685. [PubMed: 22262657]
22. Boes M, Esau C, Fischer MB, Schmidt T, Carroll M, and Chen J. 1998. Enhanced B-1 cell development, but impaired IgG antibody responses in mice deficient in secreted IgM. J Immunol 160: 4776–4787. [PubMed: 9590224]
23. Papeta N, Zheng Z, Schon EA, Brosel S, Altintas MM, Nasr SH, Reiser J, D'Agati VD, and Gharavi AG. 2010. Prkdc participates in mitochondrial genome maintenance and prevents Adriamycin-induced nephropathy in mice. J Clin Invest 120: 4055–4064. [PubMed: 20978358]
24. Pierangeli SS, and Harris EN. 2008. A protocol for determination of anticardiolipin antibodies by ELISA. Nature protocols 3: 840–848. [PubMed: 18451792]
25. Renner B, Laskowski J, Poppelaars F, Ferreira VP, Blaine J, Antonioli AH, Hannan JP, Kovacs JM, van Kooten C, You Z, Pickering MC, Holers VM, and Thurman JM. 2022. Factor H related proteins modulate complement activation on kidney cells. Kidney Int 102: 1331–1344. [PubMed: 36063874]
26. Wang Y, Wang YP, Tay YC, and Harris DC. 2000. Progressive Adriamycin nephropathy in mice: sequence of histologic and immunohistochemical events. Kidney Int 58: 1797–1804. [PubMed: 11012915]
27. Lenderink AM, Liegel K, Ljubanovic D, Coleman KE, Gilkeson GS, Holers VM, and Thurman JM. 2007. The alternative pathway of complement is activated in the glomeruli and tubulointerstitium of mice with Adriamycin nephropathy. Am J Physiol Renal Physiol 293: F555–564. [PubMed: 17522263]
28. Kim SJ, Gershov D, Ma X, Brot N, and Elkon KB. 2003. Opsonization of apoptotic cells and its effect on macrophage and T cell immune responses. Ann N Y Acad Sci 987: 68–78. [PubMed: 12727625]
29. Nguyen TT, Elsner RA, and Baumgarth N. 2015. Natural IgM Prevents Autoimmunity by Enforcing B Cell Central Tolerance Induction. J Immunol 194: 1489–1502. [PubMed: 25595791]
30. Boes M, Schmidt T, Linkemann K, Beaudette BC, Marshak-Rothstein A, and Chen J. 2000. Accelerated development of IgG autoantibodies and autoimmune disease in the absence of secreted IgM. Proc Natl Acad Sci U S A 97: 1184–1189. [PubMed: 10655505]
31. See SB, Aubert O, Loupy A, Veras Y, Lebreton X, Gao B, Legendre C, Anglicheau D, and Zorn E. 2018. Post-Transplant Natural Antibodies Associate with Kidney Allograft Injury and Reduced Long-Term Survival. J Am Soc Nephrol 29: 1761–1770. [PubMed: 29602833]
32. Webster SE, Ryali B, Clemente MJ, Tsuji NL, and Holodick NE. 2022. Sex Influences Age-Related Changes in Natural Antibodies and CD5(+) B-1 Cells. J Immunol 208: 1755–1771. [PubMed: 35256511]
33. Jones RB, Tervaert JW, Hauser T, Luqmani R, Morgan MD, Peh CA, Savage CO, Segelmark M, Tesar V, van Paassen P, Walsh D, Walsh M, Westman K, and Jayne DR. 2010. Rituximab versus cyclophosphamide in ANCA-associated renal vasculitis. N Engl J Med 363: 211–220. [PubMed: 20647198]
34. Fervenza FC, Appel GB, Barbour SJ, Rovin BH, Lafayette RA, Aslam N, Jefferson JA, Gipson PE, Rizk DV, Sedor JR, Simon JF, McCarthy ET, Brenchley P, Sethi S, Avila-Casado C, Beanlands H,

Lieske JC, Philibert D, Li T, Thomas LF, Green DF, Juncos LA, Beara-Lasic L, Blumenthal SS, Sussman AN, Erickson SB, Hladunewich M, Canetta PA, Hebert LA, Leung N, Radhakrishnan J, Reich HN, Parikh SV, Gipson DS, Lee DK, da Costa BR, Juni P, Cattran DC, and M. Investigators. 2019. Rituximab or Cyclosporine in the Treatment of Membranous Nephropathy. N Engl J Med 381: 36–46. [PubMed: 31269364]

Key Points:

1. The absence of sIgM is associated with increased anti-cardiolipin IgG levels
2. Higher anti-cardiolipin IgG associates with worse injury in Adriamycin nephropathy
3. IgG from female *sIgM*$^{-/-}$ mice binds to injured kidney cells

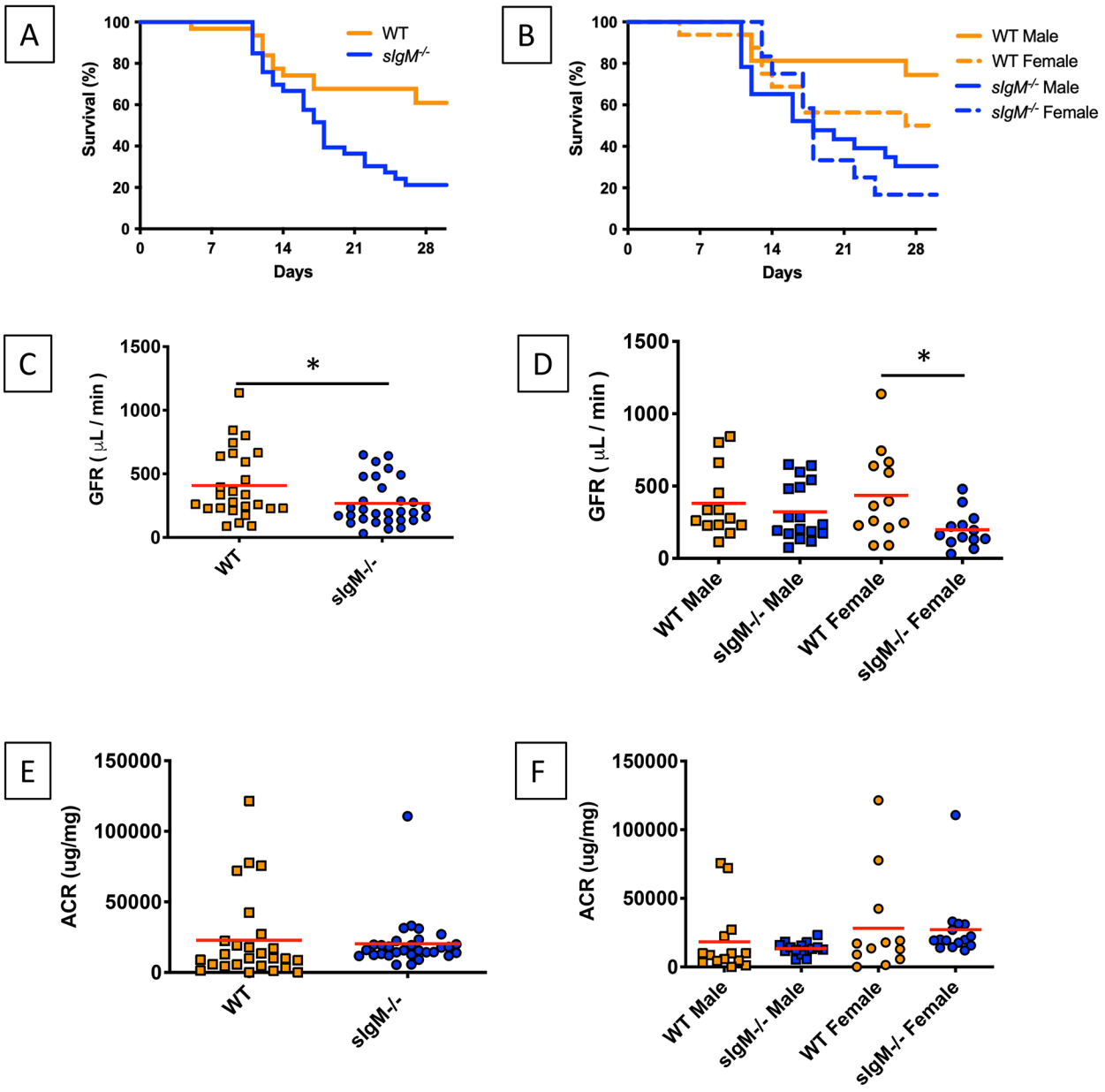

Figure 1. Mice deficient in soluble IgM are more susceptible to Adriamycin nephropathy than wild-type controls.

We induced Adriamycin nephropathy in mice that cannot produce soluble IgM (*sIgM*$^{-/-}$ mice) and age-matched Balb/c control mice. A) Greater numbers of *sIgM*$^{-/-}$ than wild-type (WT) mice died over four weeks after injection with Adriamcyin. Thirty Balb/c mice (15 males, 15 females) and 31 *sIgM*$^{-/-}$ mice (20 male, 11 female) were studied in two separate experiments. $P < 0.01$ WT versus *sIgM*$^{-/-}$. B) Mortality was greater in the female *sIgM*$^{-/-}$ mice than in the male mice, although the difference between the sexes was not statistically significant. C) One-week post-injection with Adriamycin, the glomerular filtration rates (GFRs) in the *sIgM*$^{-/-}$ mice (17 male and 13 female) were lower than in WT mice (13 male and 13 female) in three separate experiments. *$P < 0.05$. D) The GFRs in female *sIgM*$^{-/-}$ mice were significantly lower than in wild-type female mice. *$P < 0.05$. E) At one-week

post-injection with Adriamycin the urine albumin to creatinine ratios (ACRs) in the two strains of mice were not significantly different. F) There was trend towards higher ACRs in the female *sIgM*$^{-/-}$ mice compared to the male mice, but this did not reach statistical significance. The mean of each group is shown with a red line.

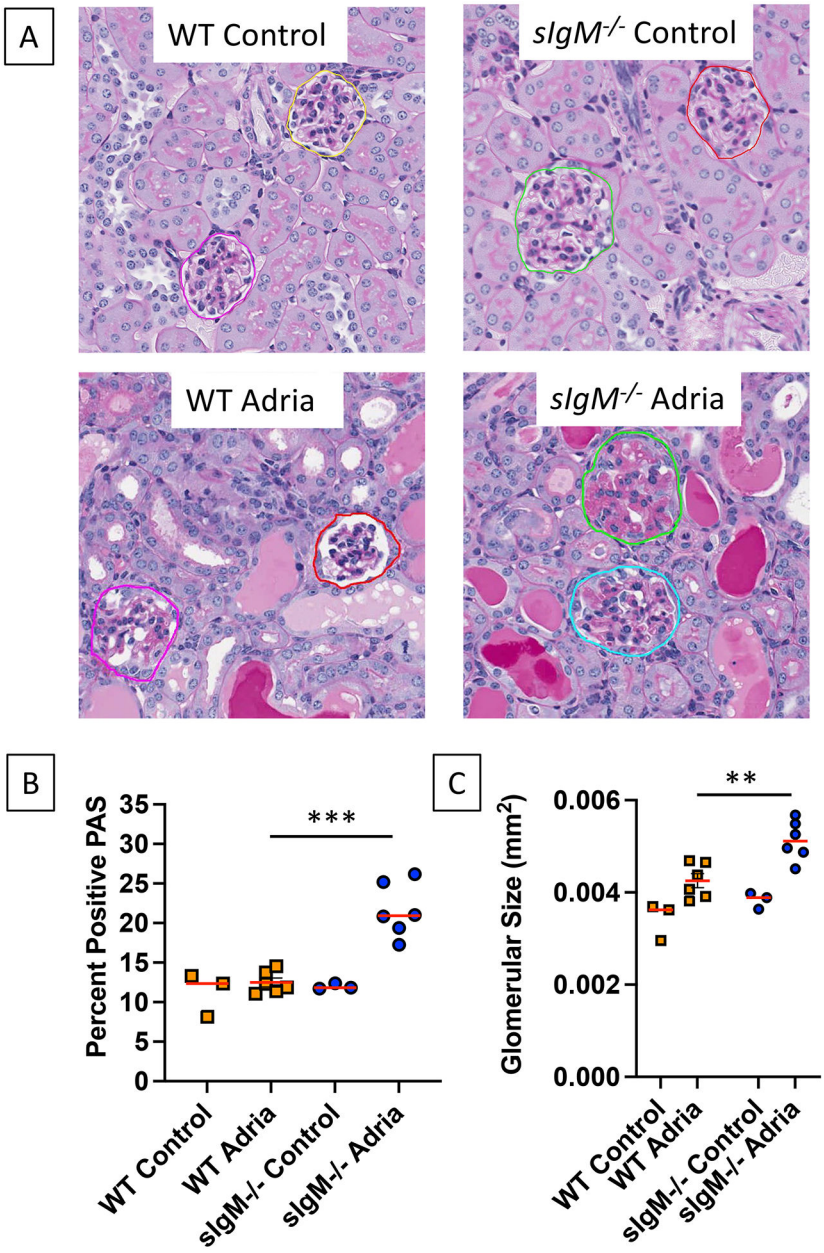

Figure 2. Female mice deficient in soluble IgM develop greater histologic injury in the kidneys after injection with Adriamycin than wild-type controls.

We induced Adriamycin nephropathy in mice that cannot produce soluble IgM (*sIgM*$^{-/-}$ mice) and in age-matched Balb/c wild-type (WT) mice, and mice were sacrificed one-week post-injection with Adriamycin. A) Periodic acid Schiff (PAS) stained kidneys from female WT (n=3 for control and n=6 adria) and *sIgM*$^{-/-}$ mice (n=3 for control and n=6 adria) were examined. The colored circles around individual glomeruli indicate representative masks that were drawn to measure PAS positive material and glomerular size. Original magnification x200. B) A greater amount of PAS-positive material was deposited in the glomeruli of soluble *sIgM*$^{-/-}$ mice than in wild-type mice. ***P < 0.001 C) The average

glomerular size in the *sIgM*$^{-/-}$ mice was greater than in WT mice. The mean of each group is shown with a red line. **P < 0.01

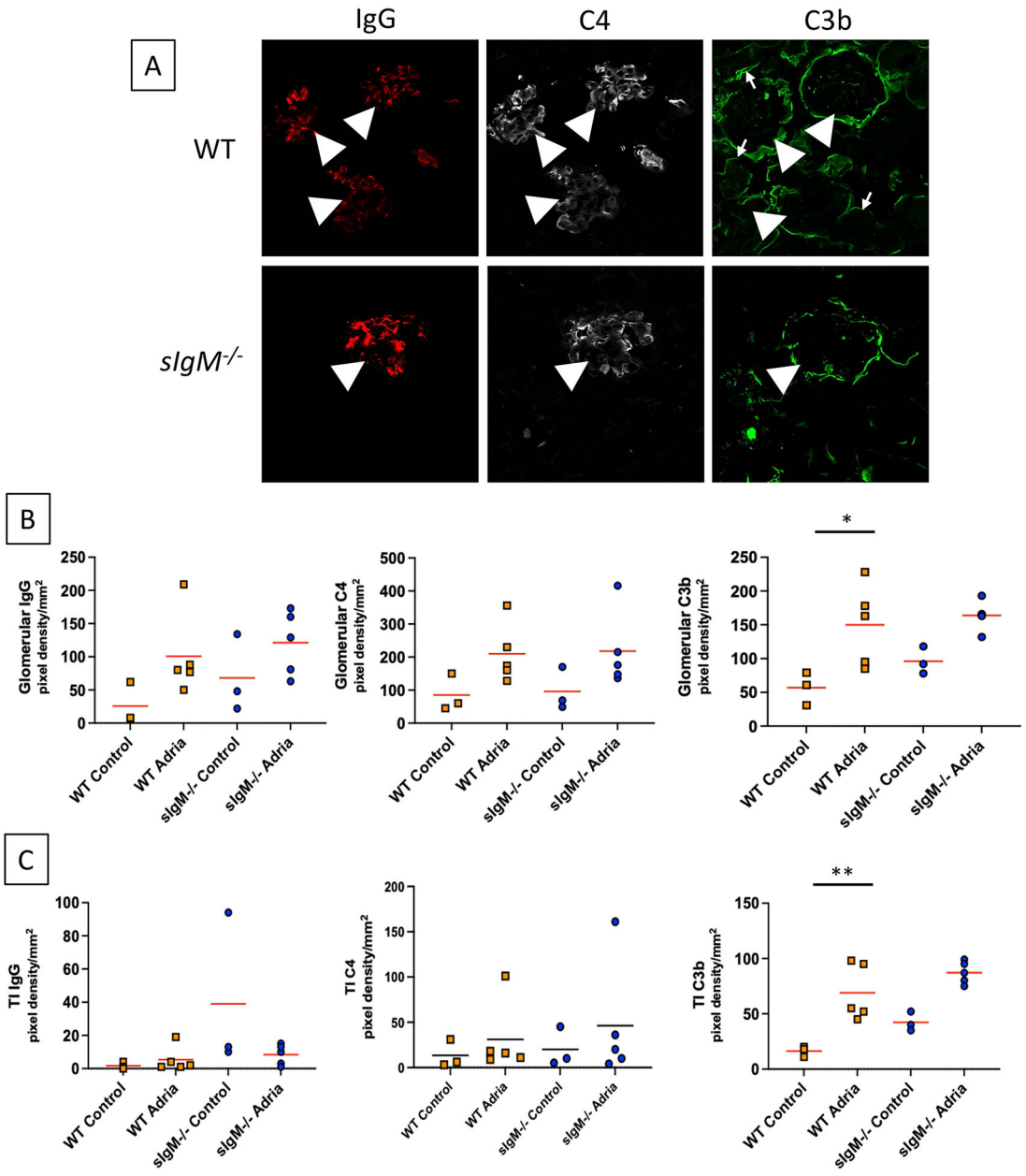

Figure 3. IgG and complement are deposited in the glomeruli of mice with Adriamycin nephropathy.

(A) We immunostained kidneys from mice that cannot produce soluble IgM (*sIgM*$^{-/-}$ mice) and Balb/c wild-type (WT) mice for IgG, C4, and C3b. For both strains of mice we included kidneys from three mice treated with PBS and five mice treated with Adriamycin. For each sample, twenty fields of view were examined in the tubulointerstitium and 15-38 glomeruli were examined based on the number available in the sample. All three proteins were detected in the glomeruli of both strains of mice. C3b was also seen on Bowman's capsure and in the tubulointerstitium. Original magnification x200. Representative images are shown, and the glomeruli are indicated with arrowheads. Fluorescence was quantified in the (B) glomeruli and (C) tubulointersitium of the tissue samples are are reported as pixel

density per μm^2. All of the proteins tended to increase after injection with Adriamycin in both strains of mice. The mean of each group is shown with a red line. *P < 0.05, **P < 0.01.

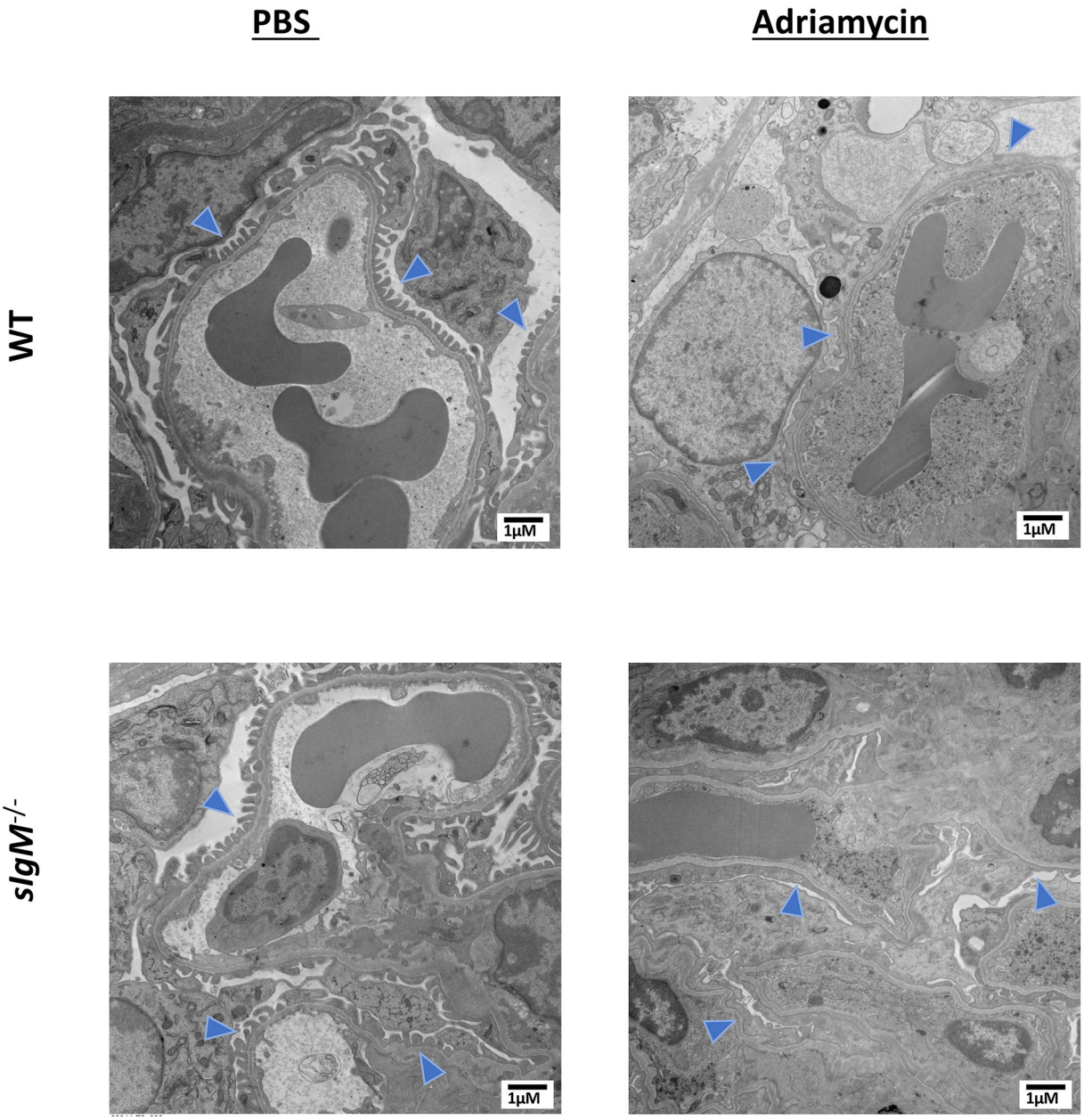

Figure 4. Wild-type and *sIgM*$^{-/-}$ glomeruli demonstrate significant podocyte injury with Adriamycin nephropathy.

(A, C) Kidneys of wt and *sIgM*$^{-/-}$ female mice treated with PBS demonstrated normal morphology, with interdigitated and morphologically intact foot processes (arrowheads), as well as intact intraluminal epithelial and capillary spaces. Three kidneys were examined for each strain, and 15-119 fields of view were examined on each sample. (B, D) Kidneys of wild-type (WT) and *sIgM*$^{-/-}$ female mice treated with Adriamycin displayed widespread foot process effacement (arrowheads), podocyte contraction and condensation. Three kidneys were examined for each strain, and 9-64 fields of view were examined on each sample.

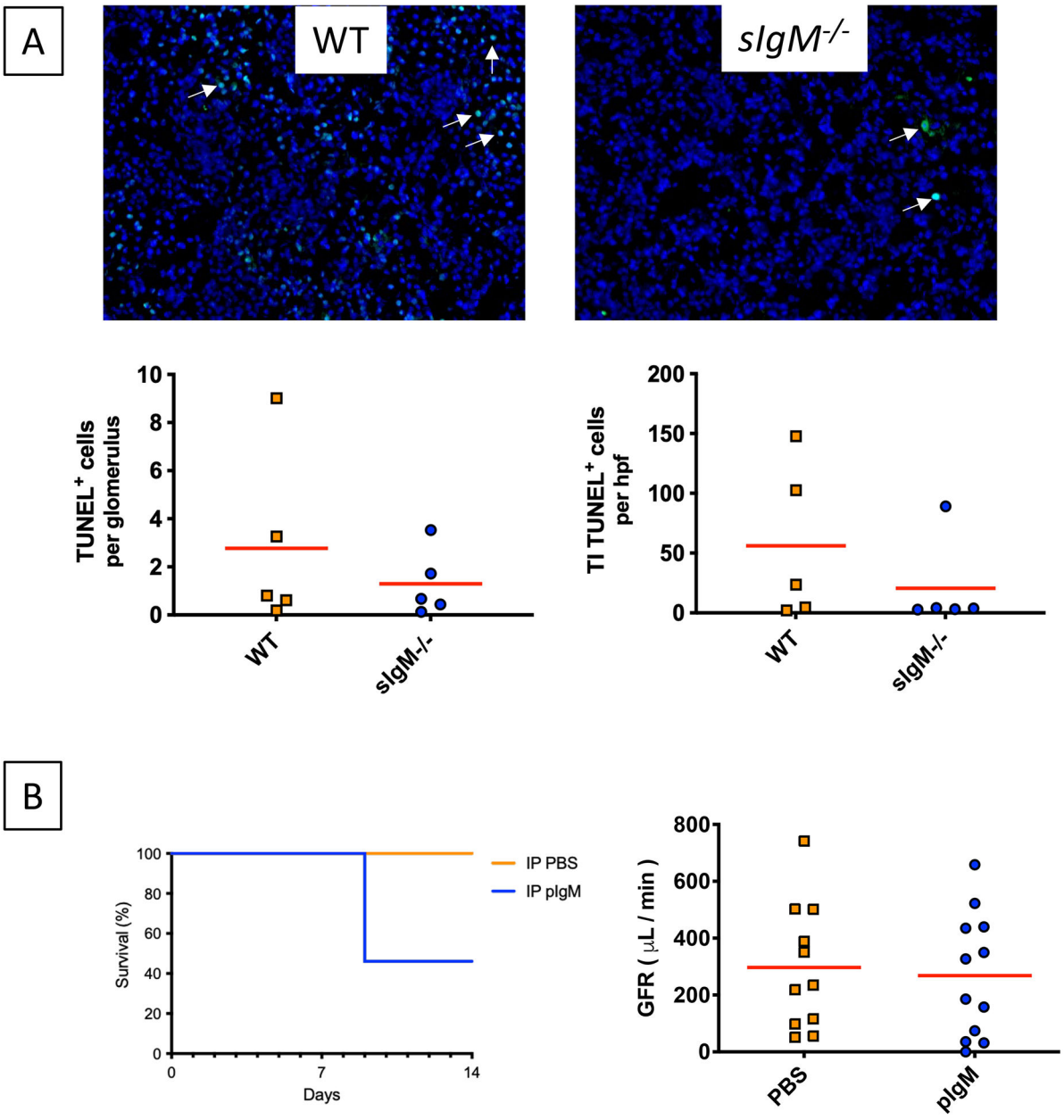

Figure 5. Soluble IgM does not reduce the number of apoptotic cells in the kidneys of mice with Adriamycin nephropathy.

A) We performed Terminal deoxynucleotidyl transferase dUTP nick end labeling (TUNEL) staining on kidney sections from female mice that cannot produce soluble IgM (*sIgM*$^{-/-}$ mice; n=5) and Balb/c wild-type (WT; n=5) mice. Four fields of view were captured at 200x magnification, and TUNEL positive cells in the glomeruli and tubulointerstitium of each field were counted. The number of TUNEL positive cells was not greater in the *sIgM*$^{-/-}$ mice compared to WT mice. Representative views are shown. (B) We reconstituted *sIgM*$^{-/-}$ mice with phosphate buffered saline (PBS; n=11) or purified IgM (n=12) to see if IgM would protect the mice from injury. Injection of the mice with IgM did not have a beneficial

effect on either survival or glomerular filtration rate (GFR). The mean of each group is shown with a red line.

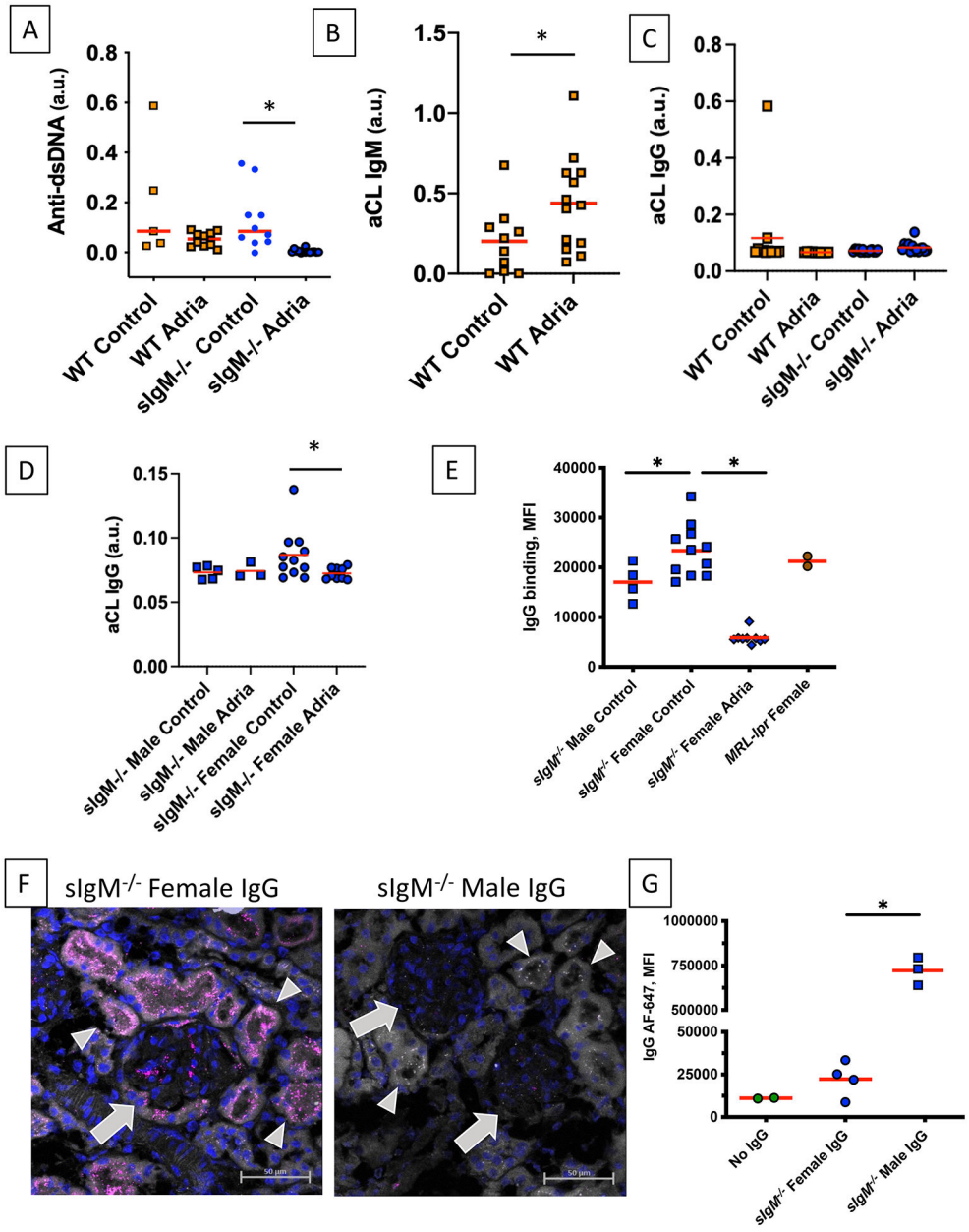

Figure 6. Female mice deficient in soluble IgM develop autoantibodies that react with kidney surfaces.

(A) We measured anti-double stranded DNA (anti-dsDNA) antibodies in serum from mice that cannot produce soluble IgM (*sIgM*$^{-/-}$ mice; n=10 control and n=14 Adria) and Balb/c wild-type (WT; n=5 control and n=10 Adria) mice. Levels were similar in the two strains at baseline. The level decreased after induction of Adriamycin nephropathy in the *sIgM*$^{-/-}$ mice. *P < 0.05, a.u.-arbitrary units. (B) Levels of anti-cardiolipin IgM increased in WT mice after induction of Adriamycin nephropathy (n=10 control and n=13 Adria). *P < 0.05 (C) Anti-cardiolipin IgG levels were similar in serum from *sIgM*$^{-/-}$ mice (n=14 control and n=14 Adria) and WT mice (n=12 control and n=10 Adria) when the male and female results were pooled. (D) When levels of anti-cardiolipin IgG were separately analyzed in male (n=5

control and n=3 Adria) and female (n=11 control and n=9 Adria) *sIgM*$^{-/-}$ mice the level in female mice decreased markedly after induction of Adriamycin nephropathy. The mean of each group is shown with a red line. *P < 0.05. (E) Mouse glomerular endothelial cells were exposed to serum, then IgG bound to the surface of the cells was evaluated by flow cytometry. At baseline, greater IgG was seen in using serum from *sIgM*$^{-/-}$ control females (n=11) compared to males (n=4), but there was a significant reduction in cell-binding IgG when serum from females treated with Adriamycin (n=9) was used. *P < 0.05. Serum from MRL-*lpr* mice was used as a reference for IgG binding (n=2). (F) Immunofluorescence was performed on wild-type female mice initially treated Adriamycin at day 0, and then injected AlexaFluor-647-labeled IgG purified from either male (n=3) or female (n=4) *sIgM*$^{-/-}$ mice at day 6, and sacrificed on day 7. Two mice that were not injected with IgG were used as controls. IgG deposition, as shown with magenta staining, is seen within the glomeruli (arrows) and proximal tubules (arrowheads) of kidneys receiving female *sIgM*$^{-/-}$ derived IgG, with minimal IgG deposition in kidneys receiving male *sIgM*$^{-/-}$ derived IgG. Blue staining is DAPI, gray staining is autofluoesence in the FITC channel to highlight kidney structure. Original magnification x400. A minimum of three fields of view and 20 glomerui were inspected, and representative pictures are shown. (G) Analysis of serum from mice injected with labeled IgG demonstrated that there was little residual IgG from female *sIgM*$^{-/-}$ mice at the time of sacrifice, whereas IgG derived from male *sIgM*$^{-/-}$ mice was still present in the serum at higher levels. Each sample was run in triplicate, and the mean for each individual mouse is plotted on the graph. *P < 0.05.